ICSV14
Cairns • Australia
9-12 July, 2007

POSITION DEPENDENT LINEARIZED ELASTIC MODELS OF PARALLEL ROBOT SYSTEMS WITH EMBEDDED SMART DEVICES FOR VIBRATION SUPPRESSION CONTROL ALGORITHMS

Michael Rose[1]*, Stephan Algermissen[1], Ralf Keimer[1], Christoph Budde[2]

[1]Institute of Composite Structures and Adaptive Systems
German Aerospace Center (DLR), Germany

[2]Institute of Machine Tools and Production Technology
Technical University Braunschweig, Germany

michael.rose@dlr.de

Abstract

The achievable accelerations of serial robot systems are limited by the weight of the axis drives, which are moved while traversing the given trajectory of the manipulator. By switching to parallel robot systems, it is possible to mount all drives on the rigid base platform. This reduction in weight of the movable linkage increases the possible accelerations, while retaining suitable position accuracy. Much weight can be reduced further on by using composite fibre materials for cranks and rods of each parallel linkage. Such systems are light and stiff and enable low cycle times, but unfortunately they are usually poorly damped as elastic structures and therefore tend to perform unwanted elastic vibrations during motion.

In this paper, position dependent models are investigated, which are suitable to generate linearized elastic system models at arbitrary positions in the work space of the robot structure. These models are further modified to include active piezo electric patch devices as actuators and sensors, which can be used to control and observe the elastic structural deformations. The final electro-mechanical coupled system model can be used to develop and simulate state space vibration control algorithms.

1. INTRODUCTION

The results presented in this paper are but a small part of ongoing work on robotic systems for handling and assembly done by a Collaborative Research Center (Sonderforschungsbereich 562). For a more complete overview of the research see references [1, 2, 3].

2. 4-DOF MECHANISM TRIGLIDE

2.1. Structural Concept

In figure 1 a TRIGLIDE mechanism is shown, which is a 3-DOF system comprised of three linear drives connected with the tool-center-point (TCP). This mechanism combined with an additional rotational axis results in a robot with 4-DOF, which is suitable for tasks of handling and assembly. Parallel kinematics in principle show a lower ratio between work and installation

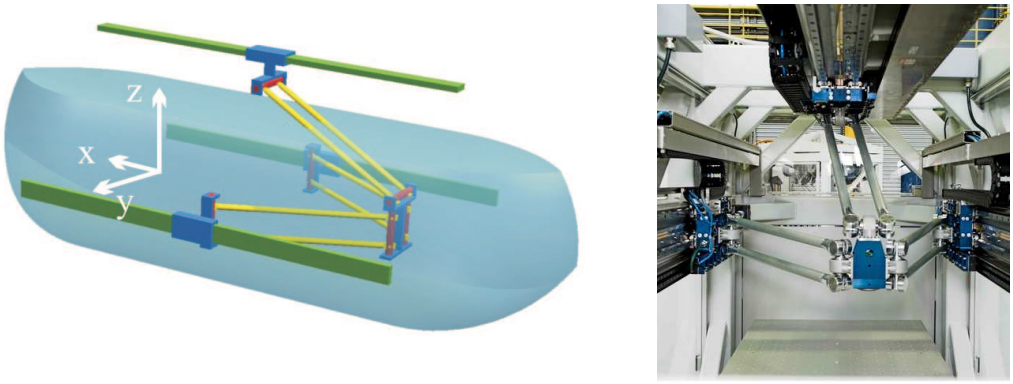

Figure 1. Triglide Mechanism. Left side shows combined workspace of two configurations, right side shows the realized demonstrator TRIGLIDE.

space compared to the more common serial kinematics used in handling and assembly. The presented demonstrator TRIGLIDE is designed in a way to overcome this problem by designing the structure so that a change between different configurations of the parallel kinematics is possible, thus combining the work spaces of the different configurations to a usable sum of work spaces as shown in figure 1 (Budde [4]). The TRIGLIDE is capable of reaching accelerations up to 10 times acceleration of gravity with a payload of up to 3 kg. In order to exploit the potential for short cycle-times in handling and assembly a vibration suppression using smart structures technologies is designed.

2.2. Components for Active Vibration Suppression

As components for vibration suppression active rods are implemented into the links of the structure. Instead of using discrete piezostack actuators as presented in earlier papers [5, 6], patch actuators as shown in figure 2 are used. The advantage of using this kind of embedded actuators lies in the integrated prestressing of the brittle piezomaterial, so that a complicated prestressing mechanism needed for discrete piezostack-actuators is not required. The combination with fiber composite material leads to an easy dimensioning of the rods against the loads induced by the handling and assembly processes. Using the design principle of Keimer [7], active rods for the TRIGLIDE were designed, which are shown in figure 2. A free stroke of 35 μm was realized using embedded actuators with a ceramic layer of 0.2 mm. The resulting fiber orientation is 45° with a wall thickness of the carbon-fiber structure of 1.5 mm with a given inner diameter of 25 mm. The weight of the active rod of 456 mm length is app. 150 g, thus being lighter than the passive aluminum rod as shown in figure 1.

Figure 2. Active rods for the TRIGLIDE: The left side depicts the embedded piezo-actuator and the finished rod, the right side shows a complete link including electrical connections of the actuators.

3. CONTROL ASPECTS AND EXPERIMENTAL RESULTS

The dimensioned rods are built into a complete TRIGLIDE-structure mounted in a frame as shown in Fig. 3. Parallel kinematics expose the problem that they have changing structural stiffness with changing position in work space, which complicates vibrational control of the structure. For vibrational control a robust control strategy (described in Zhou [8] and with more

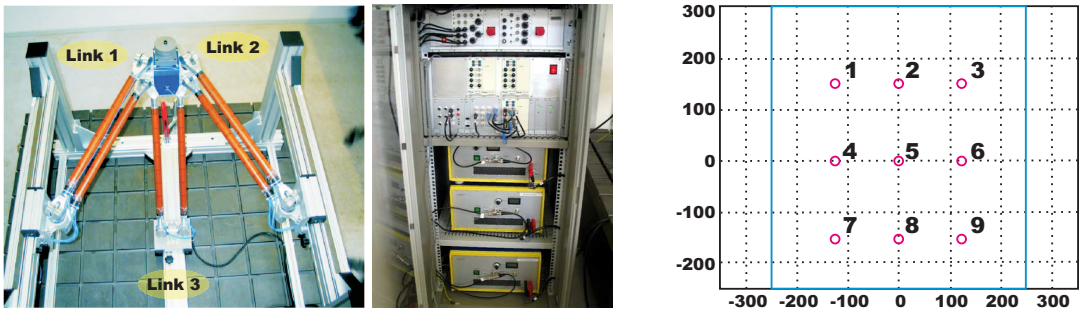

Figure 3. Left side shows the active frame mounted TRIGLIDE-structure, mid side depicts the controller cabinet with piezo amplifiers and filters and right side shows reference points in the Y-Z plane.

details regarding the particular problems of parallel mechanisms in Algermissen [9, 10]) is used. For the TRIGLIDE-structure the mechanical behaviour is uniform for every X-position but non-uniform for different Z-Y positions with respect to the given coordinate system in Fig. 1. This non-uniformity is documented by the first two plots in figure 4 where the frequency-response functions of different actuators to the measured acceleration at the TCP at reference point 7 and 3 as given in figure 3 show varying eigenvalues. To overcome this problem the work space is segmented and different controllers for the segments were developed. Because the vibration-controller is linked to the central control of the robot as described in [11] it is possible to switch between the controllers depending on the position in work space. The effectiveness of vibration control is shown by the right plot of figure 4 for reference point 1 depicting broad band reduction of vibration. These results are obtained doing tests in the setup as shown in figure 3 while controlling vibrations in the three translational DOFs. Tests under working loads while doing handling and assembly will be done later this year, then giving the possibility to assess the impact of vibration suppression on cycle times. Further work will be done to do vibrational control of the TCP in 6 DOF, controlling also the rotational vibrations.

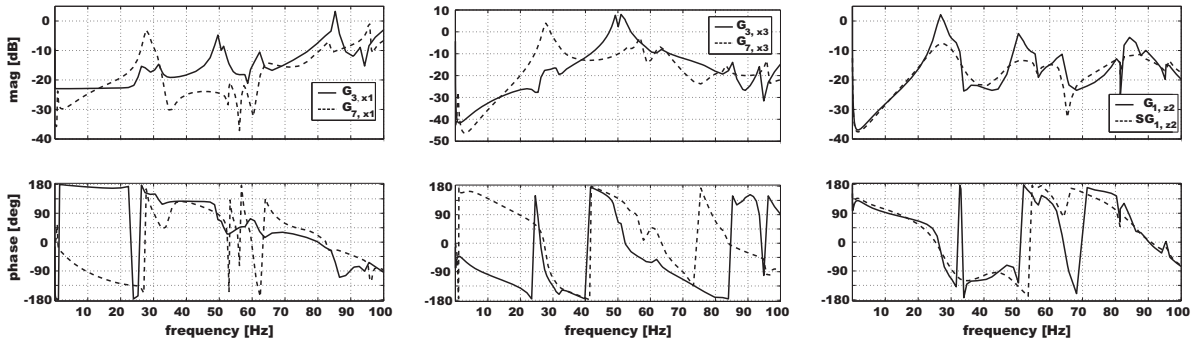

Figure 4. Left side shows frequency response function from link 1 to acceleration in X-direction, mid side from link 3 to acceleration in X-direction, both for reference point 7(slashed line) and 3(solid line), right side shows frequency response function from link 2 to acceleration in X-direction without (solid line) and with control (slashed line) for reference point 1.

4. FE-BASED ELASTIC POSITION DEPENDENT MODEL

The approach of using system identification to get a model suitable to control the elastic deformations of the robot structure has to use interpolation strategies on the workspace, to be applicable at arbitrary positions of the TCP. FE-based models with embedded non-linear kinematics can be used directly with guaranteed continuous dependency on the parameters describing the trajectory.

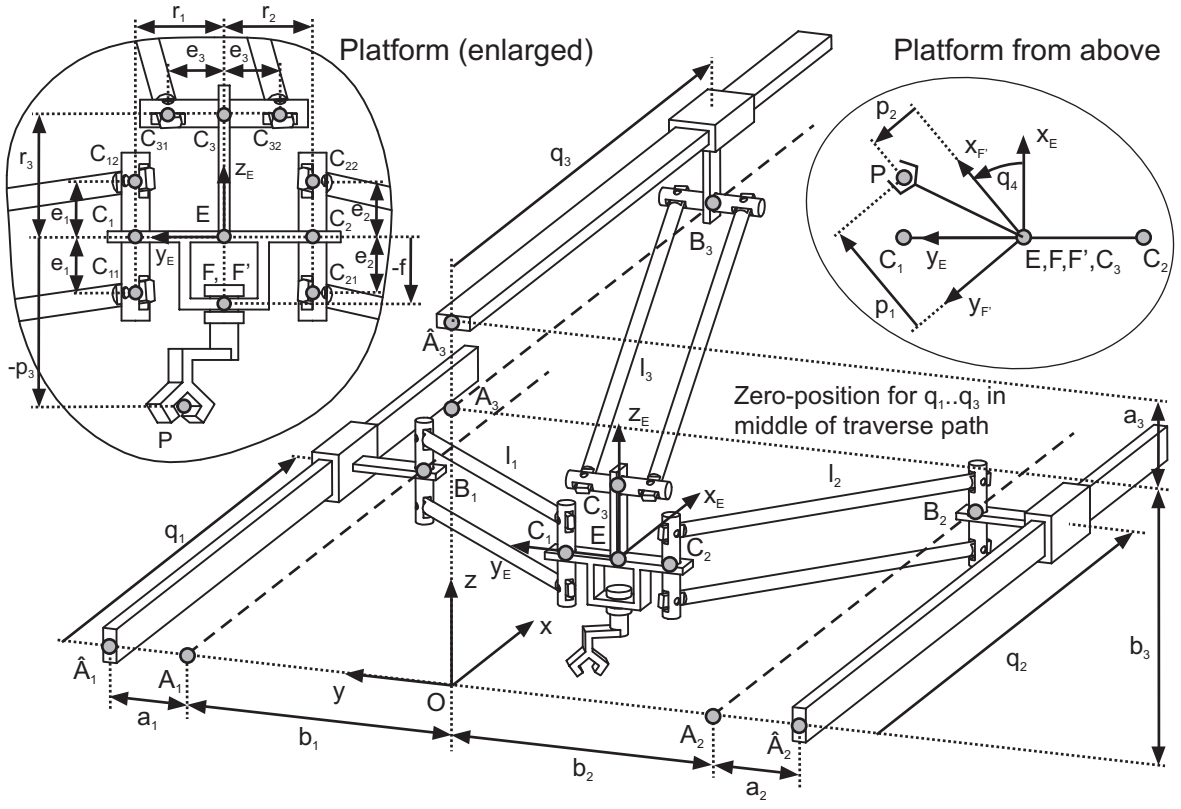

Figure 5. Schema of the TRIGLIDE-structure.

4.1. Geometric considerations

The formulation of the elastic model for the TRIGLIDE-structure needs some geometric treatment, which can be derived from figure 5, showing the most important geometric parameters. The occuring forces and moments will be described in suitable reference coordinate systems $\mathcal{O}_{P_k}$, attachted to some point P_k, which will be exactly described in the following. The most compact and exact way to describe the locations kinematically is to use transformations like $\mathcal{O}_Q = \mathcal{B} \cdot \mathcal{O}_P$, coupling the system $\mathcal{O}_Q$ with $\mathcal{O}_P$ by the transformation $\mathcal{B}$. The elementary translational and rotational transformations $\mathcal{T}_x\big[a\big]$, $\mathcal{T}_y\big[b\big]$, $\mathcal{T}_z\big[c\big]$, $\mathcal{R}_x\big[a\big]$, $\mathcal{R}_y\big[b\big]$ and $\mathcal{R}_z\big[c\big]$ will be used to describe translations and rotations with respect to the xyz-axis by the values a, b and c respectively. According to figure 5, all the neccessary reference coordinate systems can be obtained by the relations

$$
\begin{aligned}
\mathcal{O}_1 &= \mathcal{T}_y\big[-b_1 - a_1\big] \cdot \mathcal{R}_x\big[180^\circ\big] \cdot \mathcal{O}, & \mathcal{O}_{\mathrm{AS(GS)}_1} &= \mathcal{R}_y\big[180^\circ\big] \cdot \mathcal{T}_y\big[a_1\big] \cdot \mathcal{O}_{\mathrm{AS}_1},\\
\mathcal{O}_2 &= \mathcal{T}_y\big[-b_2 - a_2\big] \cdot \mathcal{O}, & \mathcal{O}_{\mathrm{AS(GS)}_2} &= \mathcal{T}_y\big[a_2\big] \cdot \mathcal{O}_{\mathrm{AS}_2},\\
\mathcal{O}_3 &= \mathcal{T}_y\big[-b_3 - a_3\big] \cdot \mathcal{R}_x\big[-90^\circ\big] \cdot \mathcal{O}, & \mathcal{O}_{\mathrm{AS(GS)}_3} &= \mathcal{T}_y\big[a_3\big] \cdot \mathcal{O}_{\mathrm{AS}_3},\\
\mathcal{O}_{\mathrm{AS}_i} &= \mathcal{T}_x\big[q_i\big] \cdot \mathcal{O}_i, & \mathcal{O}_{\mathrm{GS}_i} &= \mathcal{R}_z\big[\gamma_i\big] \cdot \mathcal{O}_{\mathrm{AS(GS)}_i},\\
\mathcal{O}_{\mathrm{GS(SP)}_i} &= \mathcal{R}_x\big[-90^\circ\big] \cdot \mathcal{T}_z\big[e_i\big] \cdot \mathcal{O}_{\mathrm{GS}_i}, & \mathcal{O}_{\mathrm{GS(SN)}_i} &= \mathcal{R}_x\big[-90^\circ\big] \cdot \mathcal{T}_z\big[-e_i\big] \cdot \mathcal{O}_{\mathrm{GS}_i},\\
\mathcal{O}_{\mathrm{SP}_i} &= \mathcal{R}_x\big[\beta_i\big] \cdot \mathcal{O}_{\mathrm{GS(SP)}_i}, & \mathcal{O}_{\mathrm{SN}_i} &= \mathcal{R}_x\big[\beta_i\big] \cdot \mathcal{O}_{\mathrm{GS(SN)}_i},\\
\mathcal{O}_{\mathrm{SP(GP)}_i} &= \mathcal{R}_y\big[180^\circ\big] \cdot \mathcal{T}_z\big[\ell_i\big] \cdot \mathcal{O}_{\mathrm{SP}_i}, & \mathcal{O}_{\mathrm{SN(GP)}_i} &= \mathcal{R}_y\big[180^\circ\big] \cdot \mathcal{T}_z\big[\ell_i\big] \cdot \mathcal{O}_{\mathrm{SN}_i},\\
\mathcal{O}_{\mathrm{GP(SP)}_i} &= \mathcal{R}_x\big[-90^\circ\big] \cdot \mathcal{T}_z\big[e_i\big] \cdot \mathcal{O}_{\mathrm{GP}_i}, & \mathcal{O}_{\mathrm{GP(SN)}_i} &= \mathcal{R}_x\big[-90^\circ\big] \cdot \mathcal{T}_z\big[-e_i\big] \cdot \mathcal{O}_{\mathrm{GP}_i},\\
\mathcal{O}_{\mathrm{GP(SP)}_i} &= \mathcal{R}_x\big[\beta_i\big] \cdot \mathcal{O}_{\mathrm{SP(GP)}_i}, & \mathcal{O}_{\mathrm{GP(SN)}_i} &= \mathcal{R}_x\big[\beta_i\big] \cdot \mathcal{O}_{\mathrm{SN(GP)}_i},\\
\mathcal{O}_{\mathrm{GP}_i} &= \mathcal{R}_z\big[\gamma_i\big]\mathcal{O}_{\mathrm{AP(GP)}_i}, & \mathcal{O}_{\mathrm{AP(GP)}_1} &= \mathcal{T}_y\big[r_1\big] \cdot \mathcal{O}_{\mathrm{AP}},\\
\mathcal{O}_{\mathrm{F}} &= \mathcal{T}_z\big[f\big] \cdot \mathcal{O}_{\mathrm{AP}}, & \mathcal{O}_{\mathrm{AP(GP)}_2} &= \mathcal{T}_y\big[r_2\big] \cdot \mathcal{R}_z\big[180^\circ\big] \cdot \mathcal{O}_{\mathrm{AP}},\\
\mathcal{O}_{\mathrm{EF}} &= \mathcal{R}_z\big[\psi\big] \cdot \mathcal{O}_{\mathrm{AP}}, & \mathcal{O}_{\mathrm{AP(GP)}_3} &= \mathcal{R}_y\big[180^\circ\big] \cdot \mathcal{T}_y\big[r_3\big] \cdot \mathcal{R}_x\big[90^\circ\big] \cdot \mathcal{O}_{\mathrm{AP}},\\
\mathcal{O}_{\mathrm{P}} &= \mathcal{T}_z\big[p_3\big] \cdot \mathcal{T}_y\big[p_2\big] \cdot \mathcal{T}_x\big[p_1\big] \cdot \mathcal{O}_{\mathrm{EF}}.
\end{aligned}
\tag{1}
$$

All parallel structures contain kinematically closed loops. Therefore to solve the underlying non-linear equations of motion, which can be obtained in a systematic way using the transformations just given, numerical solution precedures must be applied in general. In case of the TRIGLIDE-structure, the so called direct kinematical problem (DKP) with prescribed drive position parameters q_1, q_2, q_3 and $q_4 = \psi$ as well as the inverse kinematical problem (IKP) with known TCP parameters x_{P}, y_{P}, z_{P} and $\psi_{\mathrm{P}} = \psi$ from the trajectory planning module can be solved explicitly by elementary operations.

4.2. Dynamic equations for the rigid body system

The full set of dynamic equations for a rigid or elastic model of the TRIGLIDE-structure can be obtained by an application of the so called Jourdain principle [12]

$$
\sum_k \delta P_k = \sum_{i=1}^{3} \delta\dot{q}_i \, f_{q_i} + \delta\dot{\psi} \, \tau_\psi, \tag{2}
$$

which relates all internal and external virtual power in the system. Here f_{q_i} denotes the translatorical drive forces, τ_ψ the drive moment of the fourth rotational drive mounted on the TCP-platform, and the sum includes all rigid and elastic components or bodies of the system. Especially for rigid bodies with mass m, center of gravity $\boldsymbol{c}$ and inertia tensor $\boldsymbol{J}$, the virtual power is given by

$$\delta P = \begin{bmatrix} \boldsymbol{\delta v} \\ \boldsymbol{\delta \omega} \end{bmatrix}^T \left[\begin{bmatrix} m\boldsymbol{I} & m\tilde{\boldsymbol{c}}^T \\ m\tilde{\boldsymbol{c}} & \boldsymbol{J} \end{bmatrix} \begin{bmatrix} \boldsymbol{a}-\boldsymbol{g} \\ \dot{\boldsymbol{\omega}} \end{bmatrix} + \begin{bmatrix} m\tilde{\boldsymbol{\omega}}\tilde{\boldsymbol{\omega}}\boldsymbol{c} \\ \tilde{\boldsymbol{\omega}}\boldsymbol{J}\boldsymbol{\omega} \end{bmatrix} \right]. \tag{3}$$

Note that all vectors and tensors (including the earth gravitation $\boldsymbol{g}$) are used with respect to a body fixed reference system, which moves with absolute velocity $\boldsymbol{v}$, acceleration $\boldsymbol{a}$ and angular velocity $\boldsymbol{\omega}$. The swung dash operator is defined as usual by the cross product $\tilde{\boldsymbol{\omega}}\boldsymbol{c} = \boldsymbol{\omega} \times \boldsymbol{c}$. The inertia tensor $\boldsymbol{J_0}$ with respect to $\boldsymbol{c}$ can be used to calculate the inertia tensor $\boldsymbol{J} = \boldsymbol{J_0} + m\tilde{\boldsymbol{c}}\tilde{\boldsymbol{c}}^T$ of the body reference system.

From these equations and the kinematical restrictions on the position parameters and its variations, a very efficient real time C-code has been derived, which was used as dynamic model of the rigid body TRIGLIDE-structure in the computed torque control method similar as has been done before for the HEXA-structure (Hesselbach [13]). The non-linear dynamic model was also built in the multi body system SIMPACK to verify the calculated drive forces of the realtime model. In order to excite all parts of the systems, complicated three dimensional trajectories have been used as shown in figure 6. After some code debugging, finally the forces of both

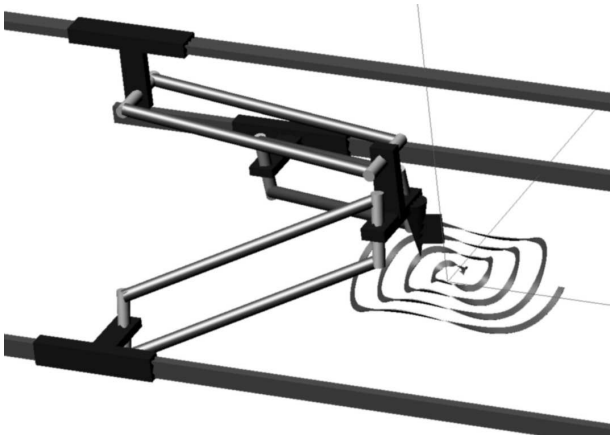

Figure 6. Example trajectory for the model verification.

models matched within floating precision.

4.3. Dynamic equations for the elastic system

To obtain an elastic model of the TRIGLIDE-structure, the rigid rods are substituted by elastic Euler-Bernoulli beams with circular cross section and the corresponding joints are supplied by discrete rotational springs and dampers. In equation (2), the virtual power $\delta P_{\text{beam},k}$ corresponding to the elastic potential of the beam and the beam mass contribution is given by

$$\delta P_{\text{beam},k} = \rho A \int_0^\ell \delta\dot{\boldsymbol{w}}(z)^T \ddot{\boldsymbol{w}}(z)\, dz + EI \int_0^\ell \delta\dot{\boldsymbol{w}}''(z)^T \boldsymbol{w}''(z)\, dz + EA \int_0^\ell \delta\dot{u}'(z) u'(z)\, dz, \tag{4}$$

with the transversal deformation $\boldsymbol{w}(z)$ and the longitudinal elongation $u(z)$. The beam is segmented and using the classical FE-approach, suitable stiffness and mass matrices are generated. In the present configuration, the active piezoceramic patches are actuated identical for each beam, which results in an equivalent external force pair $F = \alpha U$ proportional to the supplied voltage U and acting in beam direction at both ends of each beam. The appropriate actuation factor α and other parameters of this elastic formulation have been obtained by suitable FE-modells of the concrete assembly of the beams in figure 2. The external virtual power to extend the Jourdain principle in equation (2) is given by $(\delta u_k(\ell) - \delta u_k(0))\alpha U_k$. If all these equations are combined, a position dependent linearized matrix equation of the well known form

$$\boldsymbol{M_q}\ddot{\boldsymbol{u}} + \boldsymbol{D_q}\dot{\boldsymbol{u}} + \boldsymbol{K_q}\boldsymbol{u} = \boldsymbol{f} + \boldsymbol{B_q}\boldsymbol{x}, \quad \boldsymbol{y} = \boldsymbol{C_q}\ddot{\boldsymbol{u}}, \quad \boldsymbol{G_q}\boldsymbol{u} = \boldsymbol{0} \tag{5}$$

can be derived. The mass matrix $\boldsymbol{M_q}$, damping matrix $\boldsymbol{D_q}$, stiffness matrix $\boldsymbol{K_q}$ are position dependent, which is indicated by the subscript $\boldsymbol{q}$ of the drive position vector. $\boldsymbol{x}$ denotes the electric voltages applied to the individual active rods, $\boldsymbol{f}$ is a general force excitation, which includes inertia forces, $\boldsymbol{y}$ describes the accelerations of the TCP platform, which should be decreased by the vibration controller, $\boldsymbol{u}$ are the choosen finite element nodes and $\boldsymbol{G_q}$ represents the linearized equations of the kinematical constraints. By choosing some vectors $\boldsymbol{\Phi_q}$ from the kernel of $\boldsymbol{G_q}$, e.g. modal shapes from a modal analysis of equation (5), these equations can be simplified to

$$\hat{\boldsymbol{M}}_{\boldsymbol{q}}\ddot{\boldsymbol{z}} + \hat{\boldsymbol{D}}_{\boldsymbol{q}}\dot{\boldsymbol{z}} + \hat{\boldsymbol{K}}_{\boldsymbol{q}}\boldsymbol{z} = \boldsymbol{\Phi}_{\boldsymbol{q}}^T\boldsymbol{f} + \hat{\boldsymbol{B}}_{\boldsymbol{q}}\boldsymbol{x}, \quad \boldsymbol{y} = \hat{\boldsymbol{C}}_{\boldsymbol{q}}\ddot{\boldsymbol{z}}, \quad \boldsymbol{u} = \boldsymbol{\Phi_q}\boldsymbol{z} \quad \text{with} \tag{6}$$

$$\hat{\boldsymbol{M}}_{\boldsymbol{q}} = \boldsymbol{\Phi}_{\boldsymbol{q}}^T\boldsymbol{M_q}\boldsymbol{\Phi_q}, \ \hat{\boldsymbol{D}}_{\boldsymbol{q}} = \boldsymbol{\Phi}_{\boldsymbol{q}}^T\boldsymbol{D_q}\boldsymbol{\Phi_q}, \ \hat{\boldsymbol{K}}_{\boldsymbol{q}} = \boldsymbol{\Phi}_{\boldsymbol{q}}^T\boldsymbol{K_q}\boldsymbol{\Phi_q}, \ \hat{\boldsymbol{B}}_{\boldsymbol{q}} = \boldsymbol{\Phi}_{\boldsymbol{q}}^T\boldsymbol{B_q}, \ \hat{\boldsymbol{C}}_{\boldsymbol{q}} = \boldsymbol{C_q}\boldsymbol{\Phi_q}. \tag{7}$$

These models have been set up for the TRIGLIDE-structure, but they are yet not fine tuned and there is ongoing work to compare their frequency response functions with measured data. Once they fit the data, they can ease simulation studies for control performance and enhance the control layout over the workspace of the parallel robot structure.

5. CONCLUSION AND OUTLOOK

In the field of handling and assembly smart structures technologies have proven to be useful to further enhance the performance of robots. The more common approach of active vibration suppression using piezoceramic actuators could be adapted to the problems of parallel kinematics using a suitable controller design. The use of surface bonded actuators as presented in this paper proved to ease the design process of active components significantly, due to the fact that no external pre-stressing of the actuators has to be done, leading to more conventional designs. Further investigations will be done in order to do vibrational control of TCP in all DOFs. Different active components e.g. torsional actuators or bending actuators will be investigated.

The position dependent elastic model of the TRIGLIDE-structure will be adapted by FE-updating procedures to fit the frequency response curves, obtained by measurements at the specified grid positions in figure 3.

ACKNOWLEDGMENTS

The presented work was funded by the German Research Foundation (Deutsche Forschungsgemeinschaft, DFG) within the framework of the Collaborative Research Center (Sonderforschungsbereich 562) titled "Robotic Systems for Handling and Assembly — High Dynamic Parallel Structures with Adaptronic Components".

REFERENCES

[1] M. Krefft, F. M. Wahl (Edts.), “Proceedings of the First International Colloquium of the Collaborative Research Centre 562 "Robotic Systems for Handling and Assembly"”, *Fortschritte in der Robotik* **7**, Verlag Shaker, Aachen 2002, Germany, ISBN 3-8322-0201-3.

[2] P. Last, C. Budde, F. M. Wahl (Edts.), “Proceedings of the 2nd International Colloquium of the Collaborative Research Centre 562 "Robotic Systems for Handling and Assembly"”, *Fortschritte in der Robotik* **9**, Verlag Shaker, Aachen 2005, Germany, ISBN 3-8322-3866-2.

[3] http://www.tu-braunschweig.de/sfb562

[4] C. Budde, P. Last, and J. Hesselbach, “Workspace Enlargement of a Triglide Robot by changing Working and Assembly Mode”, *Proceedings of the IASTED International Conference on ROBOTICS AND APPLICATIONS*, Cambridge, USA, 2005.

[5] E. Breitbach, R. Keimer, M. Rose and D. Sachau, “An Adaptronic Solution to Increase Efficiency of High Speed Parallel Robots”, *ICAST, 12th International Conference on Adaptive Structures and Technologies*, College Park, Maryland, USA, 14-17 October, 2001.

[6] S. Algermissen, M. Rose, R. Keimer, E. Breitbach, “High-Speed Parallel Robots with Integrated Vibration-Suppression for Handling and Assembly”, *Proceedings of SPIE’s 11th Annual International Symposium on Smart Structures and Materials*, San Diego, CA, USA, 16-20 March, 2004.

[7] R. Keimer, S. Algermissen, N. Pavlovic, C. Budde, “Smart structures technologies for parallel kinematics in handling and assembly”, *Proceedings of SPIE’s 14th Annual International Symposium on Smart Structures and Materials*, San Diego, CA, USA, 2007.

[8] K. Zhou, J. C. Doyle and K. Glover, “Robust and optimal control”, Prentice-Hall, 1996.

[9] S. Algermissen, R. Keimer, M. Rose, E. Breitbach, and H. P. Monner, “Applied Robust Control for Vibration Suppression in Parallel Robots”, *Proceedings of 22nd International Symposium on Automation and Robotics in Construction (ISARC)*, 11-14 September, Ferrara, Italy, 2005.

[10] S. Algermissen, R. Keimer, M. Rose, H. P. Monner, “Robust Control for Vibration Suppression on Parallel Robot TRIGLIDE”, *Proceedings of the 10th Adaptronic Congress*, 3-4 May, Göttingen, Germany, 2006

[11] J. Steiner, N. Kohn, J.-U. Varchmin, U. Goltz, “Universal Communication Architecture for high-dynamic Robot Systems using QNX”, *Proceedings of ICARCV*, Kunming, China, 2004.

[12] R. Schwertassek, *Dynamik flexibler Mehrkörpersysteme*, 476 pages, Vieweg Verlag, Braunschweig, 1999.

[13] J. Hesselbach, C. Budde, J. Maaß, E. Breitbach, M. Rose, “Dynamic Performance Enhancement of a HEXA-Parallel-Robot Using the Computed Torque Approach”, *Proceedings of Mechatronics & Robotics*, Aachen, 1006-1011, 2004.